A Potent Vaccination Strategy that Circumvents Lymphodepletion for Effective Anti-tumor Adoptive T Cell Therapy

Hyun-Il Cho[1], **Eduardo Reyes-Vargas**[2], **Julio C. Delgado**[2], and **Esteban Celis**[1,3]

[1]Immunology Program, Moffitt Cancer Center, Tampa FL

[2]ARUP Institute for Clinical and Experimental Pathology, Department of Pathology, University of Utah School of Medicine, Salt Lake City, UT

[3]Departments of Oncologic Sciences and Molecular Medicine, University of South Florida, Tampa FL

Abstract

Adoptive cell therapy (ACT) using tumor-reactive T lymphocytes is a promising approach for treating advanced cancer. Successful tumor eradication depends primarily on the expansion and survival of the adoptively transferred T cells. Lymphodepletion using total body irradiation (TBI) and administering high dose IL2 have been used with ACT to promote T cell expansion and survival to achieve maximal therapeutic effects. However, TBI and high dose IL2 increase the risk for major complications that impact overall survival. Here we describe an alternative approach to TBI and high dose IL2 for optimizing ACT, resulting in dramatic therapeutic effects against established melanomas in mice. Administration of a potent, non-infectious peptide vaccine after ACT dramatically increased antigen-specific T cell numbers leading to enhancement in the survival of melanoma-bearing mice. Furthermore, combinations of peptide vaccination with PD1 blockade or IL2/anti-IL2 antibody complexes led to complete disease eradication and long-term survival in mice with large tumors receiving ACT. Our results indicate that PD1 blockade and IL2/anti-IL2 complexes enhance both the quantitative and qualitative aspects of the T cell responses induced by peptide vaccination after ACT. These findings could be useful for the optimization of ACT in cancer patients without the need of toxic adjunct procedures.

Introduction

CD8 T lymphocytes recognize and destroy tumor cells through perforin/granzyme B-mediated lysis or via the production of cytostatic lymphokines (1–4). Tumor-reactive CD8 T cells recognize peptide antigens that associate with major histocompatibility complex (MHC) class I molecules on the surface of tumor cells (5). In the case of malignant melanoma, peptides can be derived from melanosomal differentiation antigens such as gp100, and tyrosinase-related proteins (6–8). One factor limiting the effectiveness of T cells to recognize tumors is related to the T cell receptor (TCR) antigen affinity, which requires being sufficiently high to enable T cell activation when tumor cells express low density of peptide/MHC-I complexes (9, 10). Since in many instances normal tissues also express the tumor-associated proteins, immunological tolerance precludes the induction of T cells expressing high affinity TCRs, limiting the effectiveness of many therapeutic vaccines (11,

Corresponding author: Esteban Celis, Moffitt Cancer Center, 12902 Magnolia Drive, SRB2, Tampa, FL 33612. Tel: 813-745-1925; Fax: 813 745-7265; ecelis@moffitt.org..

12). In view of this, adoptive immunotherapy utilizing high avidity CD8 T cells has been explored to treat established and aggressive malignant diseases such as melanoma (13, 14). In addition to TCR affinity, other factors may determine the effectiveness of adoptive cell therapy (ACT), such as the ability of the T cells to expand and survive *in vivo* after adoptive transfer into the tumor-bearing hosts. Lymphokines such as IL2, IL7 and IL15 are critical for expansion and survival of T cells and generating long-lasting memory CD8 T cells (15–17). Some procedures have been used to increase the access of the transferred T cells to these lymphokines such as the co-administration of high dose IL2 (18, 19) and lymphodepletion using total body irradiation (TBI) or chemotherapy (14, 20–23). Unfortunately these procedures generate severe toxic effects that can be life threatening.

The B16 mouse melanoma model has been widely used and proven to be valuable for developing effective ACT strategies for melanoma patients (24). In this model the use of high avidity CD8 T cells obtained from Pmel-1 TCR transgenic mice was effective against large-established tumors but required lymphodepletion, high dose IL2 and active immunization using a recombinant vaccinia virus vaccine after the T cell transfers (25). Our goal was to determine whether effective ACT against established B16 melanoma could be attained in the absence of the concomitant harmful procedures (high dose IL2, live vaccines and lymphodepletion). We assessed the ability of TriVax (26), a potent, non-infectious peptide-based vaccine to elicit anti-tumor effects of adoptively transferred Pmel-1 T cells. TriVax induced significant tumor regressions in the absence of lymphodepletion and without the need of high doses of IL2. Furthermore, the addition of low dose IL2 in the form of IL2/ anti-IL2 antibody complexes (IL2Cx) or PD1 blockade to TriVax resulted in total tumor eradication. These findings may facilitate the implementation of ACT in humans in circumstances that may reduce the overall toxicity of this therapeutic approach.

Methods

Mice and cell lines

C57BL/6 (B6) mice were from Charles River (Wilmington, MA). Congenic B6 (CD45.1) and Pmel-1 mice (CD90.1) were from The Jackson Laboratory (Bar Harbor, ME). Animal care and experiments were conducted according to our institutional animal care and use committee guidelines. Murine melanoma B16F10 and RMA-S cells cells were from the American Type Culture Collection (Manassas, VA). Transfected RMA-S/CD80 cells were prepared using a cDNA plasmid encoding for the mouse CD80.

Peptides, antibodies and tetramers

Synthetic peptides representing the CD8 T cell epitopes $hgp100_{25}$ (KVPRNQDWL), $mgp100_{25}$ (EGSRNQDWL), $LCMV_{33}$ (KAVYNFATM), $Trp1_{455}$ (TAPDNLGYA), the heteroclitic analog $Trp1_{455/9M}$ (TAPDNLGYM) and Ova_{55} (KVVRFDKL) were from A&A Labs (San Diego, CA). Monoclonal anti-mouse CD40 (FGK45.5) and anti-4-1BB/CD137 (2A) were isolated from hybridoma culture supernatants. Anti-mouse programmed death ligand-1 (PD-L1; 10F.9G2), anti-mouse IL2 (JES6-5H4) and anti-mouse OX40/CD134 (OX-86) were from BioXCell (West Lebanon, NH). $H-2Db$ /$Trp1_{455}$ and $H-2Db$/$hgp100_{25}$ tetramers were provided by the NIAID Tetramer Facility (Emory University, Atlanta, GA). Fluorescent antibodies for flow cytometry were from eBioscience, Inc. (San Diego, CA).

Adoptive cell transfers and immunizations

B6 mice were injected *i.v.* with 0.3 to 3×10^6 splenocytes from naïve Pmel-1 mice. Mice were vaccinated one day after ACT. TriVax consists of 200 μg synthetic peptide, 100 μg anti-CD40 mAb (clone FKG45.5) and 50 μg poly-IC (Poly-ICLC, Oncovir, Inc., Washington, DC), which was administered as a mixture via the *i.v.* (tail vein) route. Some

mice were immunized *s.c.* with 200 μg of hgp100$_{25}$ emulsified in incomplete Freund's adjuvant (IFA/hgp100$_{25}$) or i.v. with 3×10^6 DC pulsed with 10 μg of hgp 100$_{25}$ for 18 h. Dendritic cells (DCs) were generated from bone marrow macrophages cultured for 6 days with 10 ng/mL GM-CSF and 5 ng/mL IL4 and matured with 20 ng/ml TNFα (PeproTech). For PD1 blockade, anti-PD-L1 mAb was administered *i.p.* (200 μg/dose) on days 2, 4, 6, 8 and 10 after TriVax. IL2/anti-IL2 mAb complexes (IL2Cx), were prepared by incubating 2 μg recombinant mouse IL2 with 10 μg anti-mouse IL2 (JES6-5H4) per dose for 18 h at 4 °C. IL2Cx were administered *i.p.* on days 2, 3, 5 and 7 after TriVax. For adoptive transfer using endogenous, vaccine-generated T cells, B6 mice received 3×10^6 Trp1$_{455}$-specific CD8 T cells generated in B6 mice immunized with Trp1$_{455/9M}$TriVax. CD8 T cells were purified from spleens (Miltenyi Biotec, Auburn, CA) 10 days after the second immunization, followed by culture with irradiated (60 Gy) B16 cells for 7 days in the presence of 50 IU/ml IL2 and 5 ng/ml IL7 (PeproTech, Rocky Hill, NJ). The cells used in ACT were >50% tetramer-positive for Trp1$_{455}$.

Evaluation of cellular immune responses

For measuring antigen-specific CD8 T cell responses, peripheral blood samples or splenocytes were stained with FITC- anti-MHC class II, PerCP Cy5.5- anti-CD8a, and PE-conjugated tetramers (or in some instances APC-anti-CD90.1, for Pmel-1 cells). For intracellular staining, splenocytes were incubated with 5 μg/ml peptide for 6 h at 37 °C and stained for intracellular cytokines, IL2, IFNγ and TNFα. Fluorescence was measured using a FACSCalibur flow cytometer (BD Biosciences, San Jose, CA) and analyzed using FlowJo software (Ashland, OR). To evaluate the *in vitro* T cell tumor recognition, 1×10^5 purified antigen-specific CD8 T cells (adjusted by tetramer staining) from TriVax immunized mice were co-cultured with various numbers of irradiated (60 Gy) B16 cells in 96-well plates for 2 days. Antigen-induced IFNγ was measured in culture supernatants by ELISA (eBioscience).

Anti-tumor effects

B6 mice were injected *s.c.* with 3 or 5 μ 10^5 B16 cells and 7 (or 12 days) later, they received Pmel-1 splenocytes or activated Trp1^{455} reactive T cells. The following day the mice were vaccinated and subsequently received IL2Cx or PD1 blockade as described above. Tumor growth was monitored every 3–4 days in individual tagged mice by measuring 2 opposing diameters with a set of calipers. Results are presented as the mean tumor size (area in mm2) ± SD for every treatment group at various time points until the termination of the experiment (usually when tumors in the control group reached 2 cm diameter).

Peptide/MHC-I elution and quantification

A mild acid peptide elution procedure (27) using viable cells was used to compare the amounts of mgp100$_{25}$ and Trp1$_{455}$ found on B16 cells. Briefly, 1×10^9 B16 cells were incubated at 1×10^8 cells/ml for 5 min in a mild acid buffer (131 mM Citric Acid, 66 mM Na$_2$HPO$_4$, pH 3.0). The supernatant was filtered through a 0.45 μm membrane and concentrated with SepPAKC$_{18}$ cartridges (Waters, Milford, MA). Peptides were separated on an HPLC system (Agilent Technologies, Santa Clara, CA) equipped with a C$_{18}$ column (Vydac Grace, Columbia, MD). The peptides were collected into 81 fractions that were optimized by the retention times of mgp100$_{25}$ and Trp1$_{455}$ synthetic peptides. For estimation the amounts of mgp100$_{25}$ and Trp1$_{455}$ peptides, four adjacent HPLC fractions, predicted to contain these peptides based on HPLC runs using synthetic peptides, were resuspended in culture medium and were pulsed for onto 1×10^5 RMA-S/CD80 cells. After 1 h, 3×10^5 CD8 T cells (Pmel-1 or Trp1$_{455}$ specific) were added to the peptide-pulsed RMA-S/CD80 cells and the cultures were incubated for 40 h at 37 °C. Standard curves were performed using serial dilutions of synthetic peptides mgp100$_{25}$ and Trp1$_{455}$ pulsed onto the RMA-S/

CD80 cells. Culture supernatants were assayed for IFNγ production using ELISA kits. The amounts of peptides contained in the HPLC fractions derived from the B16 cell acid eluate were estimated by measuring the amount of IFNγ produced and comparing these measurements to the values obtained in the linear portion of the synthetic peptide standard curves, taking into account dilution factors and adding the values obtained for all fractions for each peptide that stimulated the T cells.

MHC binding and stabilization assays

Peptide/MHC binding and dissociation assays were performed following similar procedures as described by van Stipdonk (28). TAP-deficient RMA-S cells were incubated with serial dilutions of various peptides for 18 h. For peptide-dependent stabilization assays, RMA-S cells were loaded with 20 µg/ml peptides for 1 h, washed, and incubated in AIM-V medium at 37 °C for various time points. After these incubations, surface expression of H-2Db was measured by flow cytometry using FITC-conjugated monoclonal antibody (28-14-8, eBioscience).

Statistical analyses

The results are representative of data obtained from at least two independent experiments. Statistical significance to assess numbers of antigen specific CD8 T cells was determined by unpaired Student's t tests. Tumor sizes between 2 populations throughout time were analyzed for significance using 2-way analysis of variance (ANOVA). All analyses and graphics were done using Prism 5.01 software (GraphPad, San Diego, CA). P-values less than 0.01 were considered to be statistically significant.

Results

Effects of vaccination in anti-tumor efficacy of ACT

Three peptide vaccination modes were compared for their ability to enhance the efficacy of ACT with Pmel-1 T cells against 7-day *s.c.* B16 tumors. Pmel-1 T cells recognize the mgp100$_{25}$ (EGSRNQDWL), H-2Db-restricted epitope expressed by B16 and normal melanocytes (25). The hgp100$_{25}$ peptide (KVPRNDQWL) function as a heteroclitic T cell epitope because it binds with higher affinity to H-2Db (29). Peptide hgp100$_{25}$ administered in IFA, did not decrease the tumor growth rate as compared to the unvaccinated mice (Fig. 1A). DCs pulsed with hgp100$_{25}$ had a modest therapeutic effect while TriVax (hgp100$_{25}$ peptide mixed with poly-IC and anti-CD40 antibody and administered *i.v.*)(26) had a substantially higher anti-tumor effect. TriVax immunization without Pmel-1 ACT had a negligible therapeutic effect.

Next we assessed the roles that each of the components of TriVax play in the generation of the antitumor effect with Pmel-1 ACT. The vaccine containing all three components (TriVax), was significantly superior to the administration of peptide alone, peptide plus poly-IC or peptide plus anti-CD40 antibody (Fig. 1B). Substitution of the hgp100$_{25}$ peptide for an irrelevant peptide (Ova$_{55}$) in TriVax slightly delayed tumor growth (compared to the no treatment control) but was clearly not as effective as hgp100$_{25}$TriVax. Moreover, the small therapeutic effect observed with TriVax Ova$_{55}$ was independent of ACT and did not enhance the expansion of the Pmel-1 cells when adoptively transferred into the tumor-bearing hosts (Fig. 1C). Measurements of the Pmel-1 cell numbers in blood at various time points showed that TriVax was the most effective vaccine in expanding the Pmel-1 cells (Fig. 1C). However, these numbers decreased substantially by days 25–35 (50–75%, respectively), which correlated with the observed resumed tumor growth (Fig. 1B). Similar experiments performed in tumor-free mice also indicated that TriVax was substantially more effective than peptide alone, peptide plus Poly-IC or peptide plus ant-CD40 antibody in

expanding Pmel-1 cells (Supplementary Fig. S1A–B). Moreover, the large decrease in Pmel-1 cell numbers observed in TriVax immunized tumor-bearing mice where the cells disappeared by day 45 (Fig. 1C) was not apparent in tumor-free mice, where more than 50% of the cells remained at a similar time point (Supplementary Fig. S1C).

Effects of IL2, PD1 blockade and T cell dose in anti-tumor efficacy of ACT

We have reported that TriVax induces massive T cell responses that are substantially higher than those generated by other modes of vaccination (26, 30). We hypothesized that the number of T cells that expand after vaccination determine the anti-tumor effects of ACT. To further increase T cell numbers we evaluated the use of IL2 in the form of IL2Cx, which have been shown to potentiate *in vivo* CD8 T cell expansion (31, 32). In addition, since it has been reported that B16 cells express PD-L1, a ligand for the inhibitory receptor PD1 found on activated T cells, we evaluated the use PD1 blockade using anti-PD-L1 antibodies (33–35). The results shown in Figure 2A indicate that in the presence of ACT, the addition of either IL2Cx or PD1 blockade increase dramatically the efficacy of TriVax, where complete tumor regressions were now attained. The improved anti-tumor effects observed in ACT with the TriVax IL2Cx (or PD1 blockade) combination were accompanied by a substantial improvement in the sustained numbers of expanded Pmel-1 cells (Fig. 2B). Interestingly, the administration of TriVax with IL2Cx or PD1 blockade in the absence of ACT had a small but significant therapeutic effect that did not correlate with the presence of endogenously generated T cells by the hgp100$_{25}$ peptide (Figs. 2A–B, open symbols).

Next, we compared three doses of Pmel-1 cells and the use of TriVax with IL2Cx or PD1 blockade for their therapeutic effects against 7-day established B16 tumors. Indeed, the number of Pmel-1 cells used for ACT correlated with the anti-tumor efficacy (Fig. 2C). However, regardless of the Pmel-1 cell dose, TriVax alone was not able to achieve complete tumor rejections. Nevertheless, the implementation of IL2Cx or PD1 blockade together with TriVax resulted in numerous tumor rejections.

The tumor size may impact the effectiveness of T cell immunotherapy. ACT using Pmel-1 cells followed by TriVax was used to treat 12-day established B16 tumors (~1 cm diameter). Under these circumstances, ACT followed by TriVax alone reduced the median tumor growth rate only by ~5 days (Fig. 3A). The addition of PD1 blockade to the therapy reduced significantly the median tumor growth rate(~22 days), but no tumor rejections were observed. In contrast, IL2Cx with TriVax resulted in tumor rejection in 80% of the mice. When the frequency of Pmel-1 cells in blood was measured it became evident that the combination using IL2Cx helped to maintain higher numbers of the adoptively transferred T cells as compared to TriVax alone or TriVax/PD1 blockade (Fig. 3B).

Effects of IL2Cx and PD1 blockade in TriVax generated responses after ACT

The above results suggest that PD1 blockade and IL2Cx therapy potentiate the efficacy of Pmel-1 ACT mostly by enhancing T cell expansion induced by TriVax. To further study this possibility we evaluated the overall expansion of adoptively transferred Pmel-1 cells induced by TriVax alone or in combination with PD1 blockade or IL2Cx in tumor-free hosts by enumerating the total numbers of Pmel-1 cells in their spleens. Seven days after TriVax immunization the Pmel-1 cells expanded ~ 20-fold (Fig. 4A). With the addition of PD1 blockade or IL2Cx to TriVax, the T cell expansion increased to 100-fold and 370-fold, respectively.

Functional assessment of the expanded Pmel-1 cells revealed that production of IFNγ, IL2 and TNFα induced by antigen stimulation was similar in mice receiving TriVax alone or combined with PD1 blockade or IL2Cx (Fig. 4B). The expression of PD1 on the T cells

could have an impact on their effectiveness against PD-L1 expressing tumor cells. Figure 4C shows that the levels of PD1 were lower on the Pmel-1 cells obtained from TriVax/IL2Cx and TriVax/PD1 blockade groups as compared to TriVax alone. The levels of PD1 in all cases were higher as compared to those observed in naïve Pmel-1 T cells. The possibility that IL2Cx and PD1 blockade could also impact the qualitative response of the adoptively transferred Pmel-1 cells after TriVax was examined. Tumor recognition by the Pmel-1 cells will have an impact in the therapeutic benefit of ACT. Pmel-1 cells from mice that received ACT/TriVax combined with either IL2Cx or anti-PD-L1 antibodies were much more effective in recognizing B16 cells *in vitro* as compared to the Pmel-1 cells obtained from mice that received TriVax alone (Fig. 4D). Thus, the addition of IL2Cx or PD1 blockade in ACT/TriVax improved both quantitatively and qualitatively the Pmel-1 response. Notably, costimulatory antibodies to OX40 and 4-1BB, which are known to enhance the magnitude and quality of T cell responses to vaccination, were not as effective as anti-PD-L1 in increasing T cell numbers or in potentiating the therapeutic effect of ACT/TriVax (Supplementary Fig. S2).

Efficacy of ACT using TriVax generated polyclonal CD8 T cells

The source of CD8 T cells for ACT in humans can vary, such as utilizing *in vitro* expanded tumor-infiltrating lymphocytes (TILs), or genetically modified CD8 T cells transduced with genes encoding TCR chains for a specific tumor epitope. Another source of antigen-specific T cells are those generated through vaccination and subsequently expanded in tissue culture prior to ACT. We explored this approach by generating antigen-specific CD8 T cells through TriVax immunization using the heteroclitic $Trp1_{455/9M}$ peptide. ACT using vaccine-derived CD8 T cells specific for the $Trp1_{455}$ epitope was effective in reducing the rate of tumor growth and the concomitant use of PD1 blockade or IL-2Cx further increased the therapeutic effect (Fig. 5A). Nevertheless, in contrast to the results obtained with Pmel-1 ACT, no complete tumor regressions were observed with the $Trp1_{455}$ ACT, even though a higher number of T cells were used for the adoptive transfers. The possibility that the $Trp1_{455}$-specific CD8 T cells failed to expand after adoptive transfer and TriVax immunization was excluded by the results showing that on day 25 post-tumor inoculation, >60% of the peripheral blood CD8 T cells in all the treated mice were $Trp1_{455}$ specific (Fig. 5B). Likewise, in a similar experiment performed in tumor-free mice, the transferred $Trp1_{455}$ T cells expanded ~6-fold after TriVax or TriVax plus PD1 blockade and combination with IL2Cx resulted in ~17-fold T cell expansion (Fig. 5C). A single $Trp1_{455/9M}$TriVax immunization, in the absence of ACT induces ~5% antigen specific CD8 T cells in blood, 6 days after vaccination and that by day 18 (corresponding to day 25-post tumor injection), these numbers decrease to ~2% (H. Cho and E. Celis, unpublished). Thus, the high responses observed in Figure 5B most likely resulted from the transferred CD8 T cells. Supporting the assumption that most of the $Trp1_{455}$-specific T cells observed after ACT and TriVax are derived from the transferred cells is the data shown in Figure 5D (the same experiment presented in Figure 5C), where it is demonstrated that all of the antigen specific cells were derived from the donor (CD45.2) mice.

As mentioned previously, it has been reported that decreasing the numbers of lymphocytes in the host, for example via TBI prior to ACT can enhance the anti-tumor therapeutic effect (20, 23). However, we observed that TBI-induced lymphodepletion, administered 1 day prior to ACT with $Trp1_{455–463/9M}$ specific CD8 T cells did not further augment therapeutic effects (Supplementary Fig. S3A) or antigen-specific CD8 T cell levels (Supplementary Fig. S3B) in the TriVax treated mice regardless of whether they received or not IL2Cx.

T cell epitope levels on tumor cells determine the effectiveness of ACT

The results presented above indicate that ACT using Pmel-1 CD8 T cells, specific for the mgp100$_{25}$ was more effective than ACT utilizing Trp1$_{455}$-specific T cells. One possibility that might explain these differences would be if the antigen avidity of the TCR transgenic Pmel-1 cells was higher than the vaccine generated Trp1$_{455}$ T cells. However, peptide titration curve comparisons between these T cells revealed that the Trp1$_{455}$-specific T cells exhibited a substantially higher avidity (~30-fold), as compared to Pmel-1 cells (Supplementary Fig. S4A). Another possible explanation for the superior therapeutic effect of Pmel-1 cells could be if the B16 cells expressed higher levels of mgp100$_{25}$/H-2Db than Trp1$_{455}$/ H-2Db. To study this possibility, MHC-I binding peptides on B16 cells were eluted with mild acid treatment and the amounts of the two T cell epitopes were measured as described in "Methods". The results indicated that ~100-fold more of mgp100$_{25}$ was obtained from the B16 acid eluates as compared to Trp1$_{455}$ (Supplementary Fig. S4B).

The peptide/MHC-I density on the B16 cells for a specific epitope will be determined by numerous factors such as peptide binding affinity for its MHC-I (36) and by the amount of peptide epitope produced by the MHC-I antigen-processing pathway. Using MHC-I stabilization assays, we compared the capacity of mgp100$_{25}$ and Trp1$_{455}$ to bind to empty H-2Db molecules expressed by RMA-S cells. Notably, Trp1$_{455}$ was ~100 times more effective in binding to H-2Db as compared to mgp100$_{25}$ and the positive control LCMV$_{33}$ (Supplementary Fig. S4C). The peptide dissociation off rate from MHC-I will also affect the cell surface density of peptide/MHC-I complexes (37). Both mgp100$_{25}$ and Trp1$_{455}$ had similar dissociation rates (Supplementary Fig. S4D). These results suggest that the higher amounts of mgp100$_{25}$/H-2Db levels on B16, as compared to the levels of Trp1$_{455}$/H-2Db are not due to stronger peptide/MHC-I binding affinity or to slower MHC-I dissociation rates of the mgp100$_{25}$ epitope.

Discussion

Although ACT represents one of the most promising modes of cancer immunotherapy, its implementation in the clinic remains challenging, and in some instances the results are suboptimal. The Pmel-1 TCR transgenic mouse has aided in the development and implementation of ACT protocols in human cancer patients. Studies by Restifo and collaborators, demonstrated that many experimental conditions play a critical role in determining the efficacy of ACT against established B16 melanoma (24, 25, 38–40). Early studies showed that vaccination using live recombinant vaccinia virus (rVV), and the administration of high dose IL2 (~6×10^6 IU, or 3.6mg/Kg/day, 4 days) were necessary for obtaining tumor rejection (25). The use of live rVV vaccines generates safety issues in humans, so it is not surprising that it has not been broadly implemented in ACT clinical protocols. On the other hand, high dose IL2 has been used in the clinic, but the systemic toxic effects that sometimes are lethal are of great concern (41, 42). Other studies demonstrated that lymphodepletion induced by TBI further increased the efficacy Pmel-1 ACT, and accordingly this procedure has been translated into the clinic (14, 21, 22). It has been proposed that TBI potentiates ACT, by increasing the access of the transferred T cells to cytokines, removing inhibitory T regulatory cells and through a gut-injured microbial translocation that releases immunostimulatory TLR ligands (20, 43).

Here we demonstrate that TriVax, a non-infectious subunit vaccine was capable of generating substantial anti-tumor effects in the Pmel-1 ACT model. When compared with peptide-pulsed DCs (currently the golden standard of the field), TriVax was more than twice as effective. Although increasing the number of Pmel-1 cells enhanced the anti-tumor efficacy, no complete tumor regressions were observed when TriVax alone followed ACT. Thus, we considered 2 additional approaches to further promote the expansion of Pmel-1

cells to achieve maximal therapeutic benefits. *In vivo* use of IL2Cx increases the expansion of antigen-stimulated CD8 T cells (32). The a main advantage of utilizing IL2Cx over IL2 is that the complexes remain for longer times in circulation, allowing the use of lower cytokine doses (0.1mg/Kg/day). Also, some anti-IL2 antibodies, such as the one we used here, block IL2 binding to CD25 (high affinity IL2R), but allow binding to CD122 (intermediate affinity IL2R), promoting the expansion of activated and memory T cells w/o expanding T regulatory cells (31). Engagement of the PD1 receptor on T cells by its ligands (PD-L1 or PD-L2) during antigen stimulation inhibits TCR activation, limiting T cell expansion (35). PD1 blockade using anti-PD-L1 mAbs improves T cell activation and function (34). Our results showed that additions of IL2Cx or anti-PD-L1 to TriVax increased TriVax driven expansion of adoptively transferred Pmel-1 cells by 10- and 4-fold, respectively, as compared to TriVax alone, and the therapeutic benefits of ACT were clearly evident, achieving in many cases complete tumor rejections. These results suggested that by simply increasing Pmel-1 numbers, using higher T cell doses for ACT or by including IL2Cx or PD1 blockade, maximal therapeutic benefit was achieved. Nevertheless, the results also showed that IL2Cx and PD1 blockade increased the qualitative potency (anti-tumor recognition and decreased PD1 expression) of Pmel-1 cells. Pmel-1 cells from mice receiving ACT/TriVax with either IL2Cx or anti-PD-L1 antibodies recognized B16 tumor cells >10-fold better than Pmel-1 cells from mice receiving TriVax alone. We do not know what specific changes in Pmel-1 cells are induced by IL2Cx or PD1 blockade, resulting in increased anti-tumor reactivity. One possible mechanism for enhancing anti-tumor recognition could be an improvement in T cell avidity by increasing expression levels of costimulatory/adhesion T cell receptors such as CD8/lck, CD2 and lmphocyte function-associated antigen-1 (LFA-1). An important observation was that the addition of IL2Cx and to some extent PD1 blockade prevented the observed loss of the Pmel-1 cells expanded by TriVax in tumor-bearing hosts, which could be explained by the reduced levels of PD1 induced by these adjuncts. Notwithstanding, the overall results indicate that the therapeutic anti-tumor potentiation induced by IL2Cx and PD1 blockade in this model of ACT followed by TriVax is derived by an enhancement of both the quantitative and qualitative aspects of the CD8 T cell response.

We also presented evidence that polyclonal, vaccine-generated CD8 T cells were effective in ACT/TriVax. However, in contrast with Pmel-1 ACT, no complete tumor rejections were obtained with the $Trp1_{455/9M}$TriVax-generated T cells with IL2Cx or PD1 blockade. The higher anti-tumor efficacy of the Pmel-1 T cells compared to the $Trp1_{455/9M}$-generated CD8 T cells may be explained the observations that B16 contained ~100-times more mgp100$_{25}$/H-2Db than $Trp1_{455}$/H-2Db complexes. We attempted to induce endogenous, vaccine-generated CD8 T cells using hgp100$_{25}$TriVax for ACT. However, the antigen avidity of the endogenous hgp100$_{25}$TriVax generated T cells was 10-fold lower as compared to the Pmel-1 cells and these cells failed to recognize tumor cells (Supplementary Fig. S5). It is likely that the Pmel-1 cells express a TCR in the high end of antigen affinity spectrum because of the procedure used to select the T cells from which the TCR genes were clones (6). Nonetheless, the therapeutic anti-tumor effects obtained in ACT using the vaccine-generated $Trp1_{455/9M}$ T cells were not meager, especially when combined with IL2Cx or PD1 blockade and offer an alternative to those instances where high affinity TCR genes are not available for transduction into effector T cells.

Supplementary Material

Refer to Web version on PubMed Central for supplementary material.

Acknowledgments

References

1. Cerottini JC, Brunner KT. Cell-mediated cytotoxicity, allograft rejection, and tumor immunity. Adv Immunol. 1974; 18:67–132. [PubMed: 4151339]

2. Lowin B, Krahenbuhl O, Muller C, Dupuis M, Tschopp J. Perforin and its role in T lymphocyte-mediated cytolysis. Experientia. 1992; 48:911–20. [PubMed: 1426142]

3. Berke G. The binding and lysis of target cells by cytotoxic lymphocytes: molecular and cellular aspects. Annu Rev Immunol. 1994; 12:735–73. [PubMed: 8011296]

4. Blankenstein T, Qin Z. The role of IFN-gamma in tumor transplantation immunity and inhibition of chemical carcinogenesis. Curr Oppin Immunol. 2003; 15:148–54.

5. Germain RN, Margulies DH. The biochemistry and cell biology of antigen processing and presentation. Annu Rev Immunol. 1993; 11:403–50. [PubMed: 8476568]

6. Overwijk WW, Tsung A, Irvine KR, Parkhurst MR, Goletz TJ, Tsung K, et al. gp100/pmel 17 is a murine tumor rejection antigen: induction of "self"-reactive, tumoricidal T cells using high-affinity, altered peptide ligand. J Exp Med. 1998; 188:277–86. [PubMed: 9670040]

7. Boon T, Coulie PG, Van den Eynde BJ, van der Bruggen P. Human T cell responses against melanoma. Annu Rev Immunol. 2006; 24:175–208. [PubMed: 16551247]

8. Slingluff CL Jr. Chianese-Bullock KA, Bullock TN, Grosh WW, Mullins DW, Nichols L, et al. Immunity to melanoma antigens: from self-tolerance to immunotherapy. Adv Immunol. 2006; 90:243–95. [PubMed: 16730266]

9. Redmond WL, Sherman LA. Peripheral tolerance of CD8 T lymphocytes. Immunity. 2005; 22:275–84. [PubMed: 15780985]

10. Mueller DL. Mechanisms maintaining peripheral tolerance. Nat Immunol. 2010; 11:21–7. [PubMed: 20016506]

11. Dudley ME, Nishimura MI, Holt AK, Rosenberg SA. Antitumor immunization with a minimal peptide epitope (G9-209-2M) leads to a functionally heterogeneous CTL response. J Immunother. 1999; 22:288–98. [PubMed: 10404430]

12. Buteau C, Markovic SN, Celis E. Challenges in the development of effective peptide vaccines for cancer. Mayo Clinic Proceed. 2002; 77:339–49.

13. Rosenberg SA, Restifo NP, Yang JC, Morgan RA, Dudley ME. Adoptive cell transfer: a clinical path to effective cancer immunotherapy. Nat Rev Cancer. 2008; 8:299–308. [PubMed: 18354418]

14. Rosenberg SA, Dudley ME. Adoptive cell therapy for the treatment of patients with metastatic melanoma. Curr Opin Immunol. 2009; 21:233–40. [PubMed: 19304471]

15. Surh CD, Sprent J. Homeostasis of naive and memory T cells. Immunity. 2008; 29:848–62. [PubMed: 19100699]

16. Boyman O, Letourneau S, Krieg C, Sprent J. Homeostatic proliferation and survival of naive and memory T cells. European journal of immunology. 2009; 39:2088–94. [PubMed: 19637200]

17. Rochman Y, Spolski R, Leonard WJ. New insights into the regulation of T cells by gamma(c) family cytokines. Nat Rev Immunol. 2009; 9:480–90. [PubMed: 19543225]

18. Dudley ME, Rosenberg SA. Adoptive cell transfer therapy. Semin Oncol. 2007; 34:524–31. [PubMed: 18083376]

19. Robbins PF, Morgan RA, Feldman SA, Yang JC, Sherry RM, Dudley ME, et al. Tumor regression in patients with metastatic synovial cell sarcoma and melanoma using genetically engineered lymphocytes reactive with NY-ESO-1. J Clin Oncol. 2011; 29:917–24. [PubMed: 21282551]

20. Gattinoni L, Finkelstein SE, Klebanoff CA, Antony PA, Palmer DC, Spiess PJ, et al. Removal of homeostatic cytokine sinks by lymphodepletion enhances the efficacy of adoptively transferred tumor-specific CD8+ T cells. J Exp Med. 2005; 202:907–12. [PubMed: 16203864]

21. Powell DJ Jr. Dudley ME, Hogan KA, Wunderlich JR, Rosenberg SA. Adoptive transfer of vaccine-induced peripheral blood mononuclear cells to patients with metastatic melanoma following lymphodepletion. J Immunol. 2006; 177:6527–39. [PubMed: 17056585]

22. Dudley ME, Yang JC, Sherry R, Hughes MS, Royal R, Kammula U, et al. Adoptive cell therapy for patients with metastatic melanoma: evaluation of intensive myeloablative chemoradiation preparative regimens. Journal of Clinical Oncology. 2008; 26:5233–9. [PubMed: 18809613]

23. Wrzesinski C, Paulos CM, Kaiser A, Muranski P, Palmer DC, Gattinoni L, et al. Increased intensity lymphodepletion enhances tumor treatment efficacy of adoptively transferred tumor-specific T cells. J Immunother. 2010; 33:1–7. [PubMed: 19952961]

24. Overwijk WW, Restifo NP. B16 as a mouse model for human melanoma. Curr Protoc Immunol. 2001; Chapter 20(Unit 20):1. [PubMed: 18432774]

25. Overwijk WW, Theoret MR, Finkelstein SE, Surman DR, de Jong LA, Vyth-Dreese FA, et al. Tumor regression and autoimmunity after reversal of a functionally tolerant state of self-reactive CD8+ T cells. J Exp Med. 2003; 198:569–80. [PubMed: 12925674]

26. Cho HI, Celis E. Optimized peptide vaccines eliciting extensive CD8 T-cell responses with therapeutic antitumor effects. Cancer Research. 2009; 69:9012–9. [PubMed: 19903852]

27. Storkus WJ, Zeh HJ 3rd, Salter RD, Lotze MT. Identification of T-cell epitopes: rapid isolation of class I-presented peptides from viable cells by mild acid elution. J Immunother Emphasis Tumor Immunol. 1993; 14:94–103. [PubMed: 7506576]

28. van Stipdonk MJ, Badia-Martinez D, Sluijter M, Offringa R, van Hall T, Achour A. Design of agonistic altered peptides for the robust induction of CTL directed towards H-2Db in complex with the melanoma-associated epitope gp100. Cancer Res. 2009; 69:7784–92. [PubMed: 19789338]

29. Gold JS, Ferrone CR, Guevara-Patino JA, Hawkins WG, Dyall R, Engelhorn ME, et al. A single heteroclitic epitope determines cancer immunity after xenogeneic DNA immunization against a tumor differentiation antigen. J Immunol. 2003; 170:5188–94. [PubMed: 12734366]

30. Assudani D, Cho HI, DeVito N, Bradley N, Celis E. In vivo expansion, persistence, and function of peptide vaccine-induced CD8 T cells occur independently of CD4 T cells. Cancer Res. 2008; 68:9892–9. [PubMed: 19047170]

31. Boyman O, Kovar M, Rubinstein MP, Surh CD, Sprent J. Selective stimulation of T cell subsets with antibody-cytokine immune complexes. Science. 2006; 311:1924–7. [PubMed: 16484453]

32. Verdeil G, Marquardt K, Surh CD, Sherman LA. Adjuvants targeting innate and adaptive immunity synergize to enhance tumor immunotherapy. Proc Natl Acad Sci U S A. 2008; 105:16683–8. [PubMed: 18936481]

33. Blank C, Brown I, Peterson AC, Spiotto M, Iwai Y, Honjo T, et al. PD-L1/B7H-1 inhibits the effector phase of tumor rejection by T cell receptor (TCR) transgenic CD8+ T cells. Cancer Res. 2004; 64:1140–5. [PubMed: 14871849]

34. Hirano F, Kaneko K, Tamura H, Dong H, Wang S, Ichikawa M, et al. Blockade of B7-H1 and PD-1 by monoclonal antibodies potentiates cancer therapeutic immunity. Cancer Res. 2005; 65:1089–96. [PubMed: 15705911]

35. Sharpe AH, Wherry EJ, Ahmed R, Freeman GJ. The function of programmed cell death 1 and its ligands in regulating autoimmunity and infection. Nat Immunol. 2007; 8:239–45. [PubMed: 17304234]

36. Sette A, Vitiello A, Reherman B, Fowler P, Nayersina R, Kast WM, et al. The relationship between class I binding affinity and immunogenicity of potential cytotoxic T cell epitopes. J Immunol. 1994; 153:5586–92. [PubMed: 7527444]

37. van der Burg SH, Visseren MJ, Brandt RM, Kast WM, Melief CJ. Immunogenicity of peptides bound to MHC class I molecules depends on the MHC-peptide complex stability. J Immunol. 1996; 156:3308–14. [PubMed: 8617954]

38. Kerkar SP, Muranski P, Kaiser A, Boni A, Sanchez-Perez L, Yu Z, et al. Tumor-specific CD8+ T cells expressing interleukin-12 eradicate established cancers in lymphodepleted hosts. Cancer Res. 2010; 70:6725–34. [PubMed: 20647327]

39. Klebanoff CA, Gattinoni L, Palmer DC, Muranski P, Ji Y, Hinrichs CS, et al. Determinants of Successful CD8+ T-Cell Adoptive Immunotherapy for Large Established Tumors in Mice. Clin Cancer Res. 2011; 17:5343–52. [PubMed: 21737507]

40. Paulos CM, Wrzesinski C, Kaiser A, Hinrichs CS, Chieppa M, Cassard L, et al. Microbial translocation augments the function of adoptively transferred self/tumor-specific CD8+ T cells via TLR4 signaling. J Clin Invest. 2007; 117:2197–204. [PubMed: 17657310]

41. Acquavella N, Kluger H, Rhee J, Farber L, Tara H, Ariyan S, et al. Toxicity and activity of a twice daily high-dose bolus interleukin 2 regimen in patients with metastatic melanoma and metastatic renal cell cancer. J Immunother. 2008; 31:569–76. [PubMed: 18528297]

42. Schwartz RN, Stover L, Dutcher J. Managing toxicities of high-dose interleukin-2. Oncology. 2002; 16:11–20. [PubMed: 12469935]

43. Paulos CM, Kaiser A, Wrzesinski C, Hinrichs CS, Cassard L, Boni A, et al. Toll-like receptors in tumor immunotherapy. Clin Cancer Res. 2007; 13:5280–9. [PubMed: 17875756]
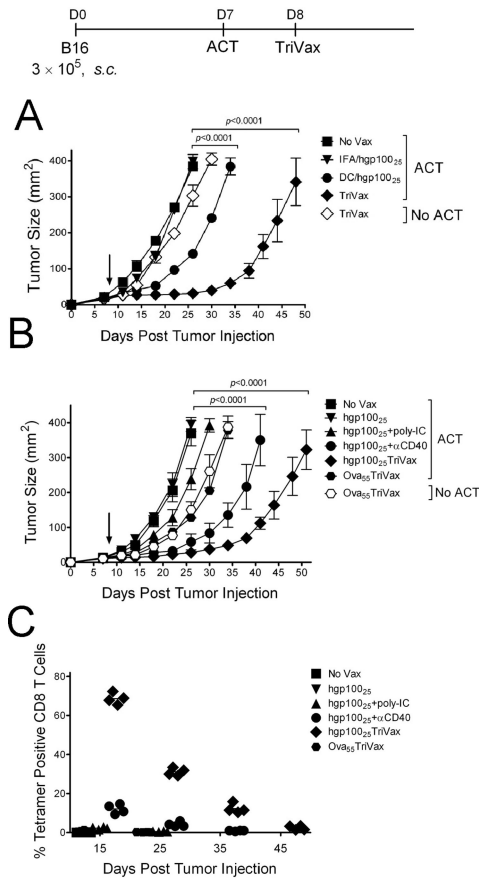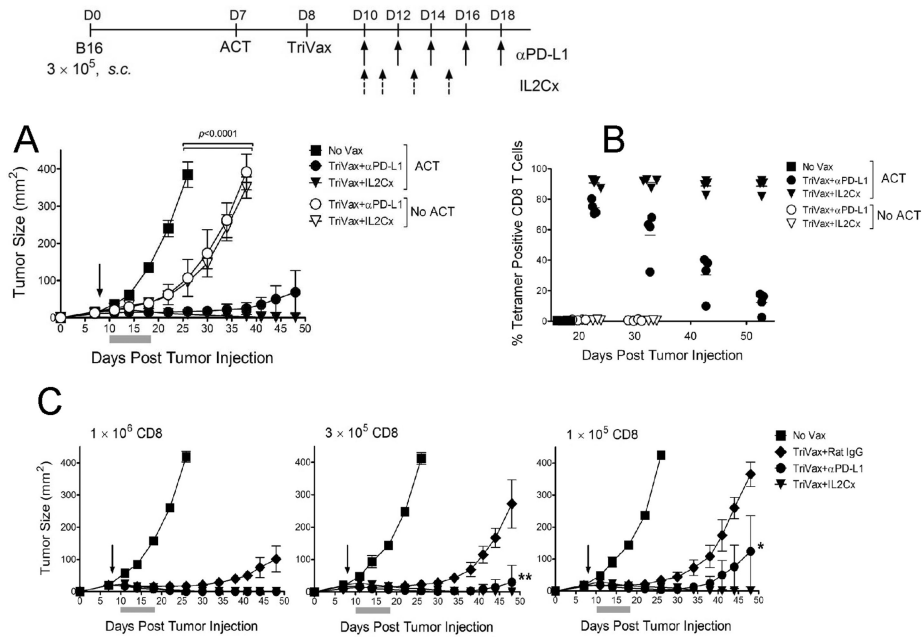
Figure 1. Effects of peptide-based vaccines on the therapeutic efficacy of ACT

(A) B6 mice (4/group) were inoculated *s.c.* on day 0 with 3×10^5 live B16 cells, and adoptively transferred on day 7 with 3×10^5 naïve Pmel-1 CD8 T cells followed by immunization on day 8 (arrow) with either TriVax, hgp100$_{25}$ in IFA, or DCs pulsed with hgp100$_{25}$. (B) Tumor-bearing mice that received ACT as described in panel A, were immunized one day later with various combinations of peptide, poly-IC and anti-CD40 mAb as indicated. Non-vaccinated mice (No Vax) and Ova$_{55}$ TriVax-vaccinated mice with and w/o ACT were included as controls. (C) Presence of antigen-specific CD8 T cells in blood observed at various time points in the mice that received ACT from the experiment in panel B. For panels A and B, tumor sizes are presented as tumor areas in mm^2. *Points* mean for each group of mice; *bars*, SD. *P* value was calculated using two-way ANOVA test comparing with the non-vaccinated group. For panel C, each symbol denotes the % tetramer positive cells related to total CD8 T cells in an individual mouse in each group.
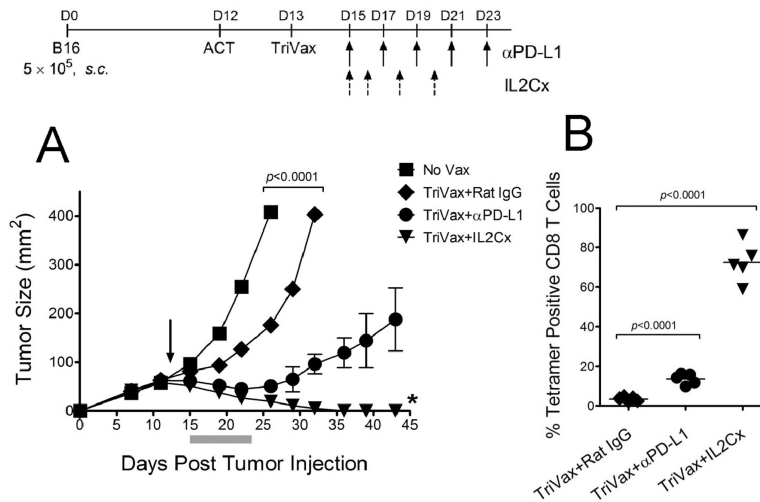
Figure 2. PD1 blockade and IL2Cx enhance the effects of TriVax, further increasing the therapeutic efficacy of ACT

(A) B6 mice (4/group) with 7-day B16 tumors received 3×10^5 Pmel-1 cells followed by TriVax on day 8 (arrow). Mice w/o ACT were also vaccinated for comparison. All mice that received ACT and treated with TriVax plus IL2Cx rejected their tumors. *P* values were calculated using two-way ANOVA. (B) Pmel-1 frequencies were evaluated by tetramer analysis using blood samples from mice in panel A. *Points*, values from each mouse; *horizontal lines*, average value of each group. (C) Tumor-bearing mice (4/group) received the indicated number of Pmel-1 cells followed by TriVax on day 8. Anti-PD-L1 mAb, normal rat IgG or IL2Cx were administered as described in "Methods". *Gray bars*, time period of PD1 blockade or IL2Cx therapy. All of the mice that received IL2Cx rejected their tumors. At the high Pmel-1 cell dose, all the anti-PD-L1 mAb treated mice rejected their tumors. **=2/4 mice in this group rejected their tumors. *=1/4 mice in this group rejected its tumor.

Figure 3. Therapeutic effects of ACT/TriVax against advanced B16 tumors
(A) B6 *s.c.* mice (5/group) were injected with 5×10^5 B16 cells, and on day 12 received 1×10^6 Pmel-1 cells followed by TriVax on day 13 (arrow) and PD1 blockade or IL2Cx. *P* values were calculated using two-way ANOVA. * = 4/5 mice rejected their tumors. (B) Antigen-specific CD8 T cells evaluated by tetramer analysis on day 25 using blood samples. *Points*, value for each mouse; *horizontal lines*, averages of the group. *P* values were calculated with unpaired Student's *t* tests.
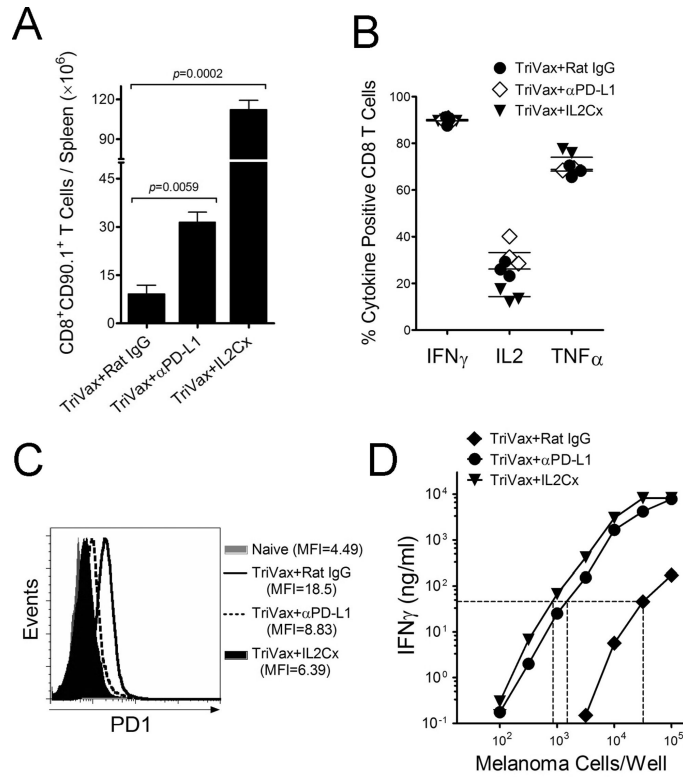
Figure 4. IL2Cx and PD1 blockade improve quantitatively and qualitatively T cell responses after ACT/TriVax

Tumor-free B6 mice (4/group) received 3×10^5 Pmel-1 cells followed by TriVax with or w/o anti-PD-L1 mAb or IL2Cx, administered as described in Figure 2A. (A) On day 14 after TriVax the total number of Pmel-1 cells (CD90.1) were enumerated in the spleens. *P* values were calculated with unpaired Student's *t* tests. (B) Antigen-induced production of cytokines evaluated by intracellular staining after stimulation with hgp100$_{25}$ peptide. *Points*, values for each mouse; *horizontal lines*, averages of each group. (C) The expression of PD-1 on Pmel-1 CD8 T cells evaluated by flow cytometry. *MFI*, median fluorescence intensity. (D) Antigen-induced IFNγ production of purified CD8 T cells evaluated by ELISA after stimulation with various numbers of B16 cells. The same number of CD8/CD90.1 cells from all treatment groups were placed in each culture. Dotted lines are for comparison on the efficacy of the various T cells to recognize the tumor cells (*i.e.*, amount of antigen required to obtain the same amount of IFNγ).
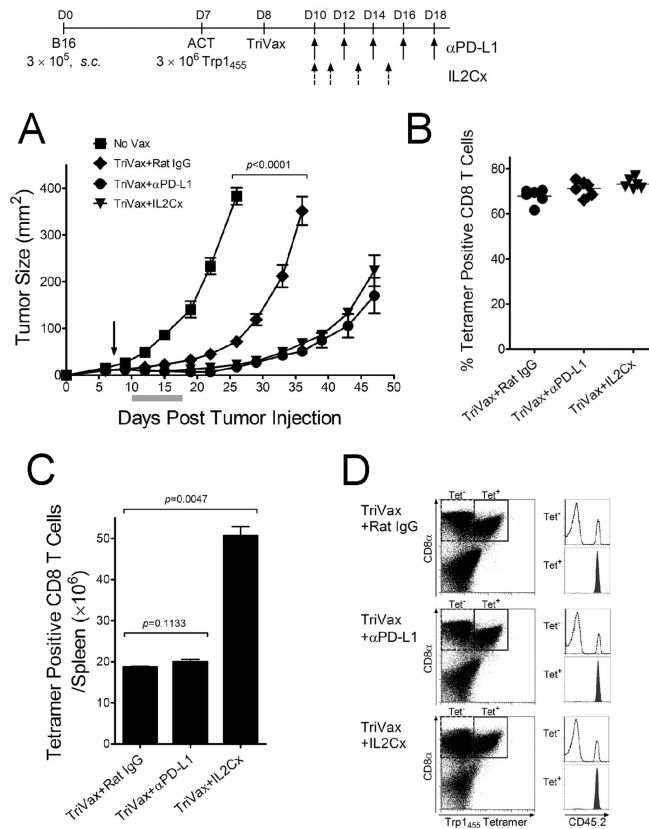
Figure 5. Anti-tumor therapeutic effects of ACT/TriVax using endogenous vaccine generated T cells

(A) B6 mice (4/group) were inoculated *s.c.* with 3×10^5 B16 cells, and adoptively transferred on day 7 with 3×10^6 Trp1$_{455}$-specific CD8 T cells followed by TriVax (arrow). PD1 blockade or IL2Cx were administered as described in the previous figures. *P* values were calculated using two-way ANOVA. (B) Frequencies of Trp1$_{455}$-specific CD8 T cells in blood samples evaluated by tetramer analysis on day 25 post-tumor inoculation. *Points*, values for each mouse; *horizontal lines*, group averages. (C) In a parallel experiment congenic CD45.1 B6 mice were adoptively transferred Trp1$_{455}$-specific CD8 T cells, generated in B6 (CD45.2) mice. 18 days later, the number of adoptively transferred CD8 T cells in spleen were estimated. *P* values calculated with unpaired Student's *t* tests. (D) Expression of CD45.2 in the tetramer positive (Tet[+]) CD8 T cells indicates that all of the antigen specific cells were derived from the donor mice.